## Spatially Assisted Schwinger Mechanism and Magnetic Catalysis

Patrick Copinger and Kenji Fukushima Department of Physics, The University of Tokyo, 7-3-1 Hongo, Bunkyo-ku, Tokyo 113-0033, Japan

[This is an erratum applied version to Phys. Rev. Lett. 117, 081603 (2016). The conclusion is not changed, but we should have considered not decreasing but increasing spatial modulations in the magnetic profile.] Using the worldline formalism we compute an effective action for fermions under a temporally modulated electric field and a spatially modulated magnetic field. It is known that the former leads to an enhanced Schwinger Mechanism, while we find that the latter can also result in enhanced particle production and even cause a reorganization of the vacuum to acquire a larger dynamical mass in equilibrium which spatially assists the Magnetic Catalysis.

Introduction: The vacuum in quantum field theory is filled with fluctuation pairs of particles and anti-particles and this fact causes various unconventional phenomena such as the Casimir force [1], the Schwinger Mechanism [2] (see Ref. [3] for a review), the spontaneous symmetry breaking, and so on. Among the above examples the Schwinger Mechanism still awaits an experimental confirmation. The idea is that particle and anti-particle (i.e.  $e^-$  and  $e^+$ ) pairs should be created from the vacuum driven by a strong external electric field E, which is analogous to the Landau-Zener effect in materials. The particle production rate w in the Schwinger Mechanism is, however, exponentially suppressed as  $w \sim e^{-\pi m_e^2/(eE)}$ . The critical electric field,  $eE_c \sim \pi m_e^2$ , is too strong to be reachable in current laboratory experiments and the detection of Schwinger pair production with strong laser fields has remained elusive (see Ref. [4] for reviews).

It is evident from such an exponential form that the electron mass could be given an interpretation as an "activation energy" in atomic ionization, and it has been concluded that the ionization is favored more by time-dependent E(t) in the pioneering work by Keldysh [5] but less by space-dependent E(x) [6]. This observation suggests that there might be an optimal profile of E(x,t) that enhances the pair production rate in the Schwinger Mechanism. Indeed, the "Dynamically Assisted Schwinger Mechanism" has been recognized by Schützhold, Gies, and Dunne [7] who first successfully quantified how much a time-dependent perturbation in the electric field can push the critical field strength down. Numerical simulations with spacetime-dependent E(x,t) have been performed later [8].

A natural question would be: What if an external magnetic field  $\boldsymbol{B}$  co-exists? For homogeneous and constant  $\boldsymbol{E}$  and  $\boldsymbol{B}$  the Euler-Heisenberg Effective Hamiltonian already contains both effects of  $\boldsymbol{E}$  and  $\boldsymbol{B}$ . In particular, if there are parallel components, i.e.  $\boldsymbol{E} \cdot \boldsymbol{B} \neq 0$ , the particle production rate w has an anomalous origin associated with the non-conservation of axial charge or the axial anomaly [9, 10]. Then, an optimal profile of  $\boldsymbol{B}(\boldsymbol{x},t)$  might further increase w. In the present work we will show that an increasing or positive curvature space-

dependent perturbation in the magnetic field decreases the effective mass of fermions and thus the critical field strength, which we call the "Spatially Assisted Schwinger Mechanism."

Such a situation with space-time modulated  $\boldsymbol{E}$  and  $\boldsymbol{B}$  would be realistic in nucleus-nucleus collisions at high energy as conducted in Relativistic Heavy-Ion Collider (RHIC) and in Large Hadron Collider (LHC). In each collision event thousands of particles (mostly pions) are created and a non-Abelian generalized Schwinger Mechanism should underlie the particle production [11, 12].

Besides, a strong B is expected in non-central collisions, which has inspired enormous activities dedicated to fermionic matter at strong constant B with lattice numerical simulations [13] and phenomenological model studies [14]. One of the most remarkable implications from the presence of such strong  $\boldsymbol{B}$  is the Chiral Magnetic Effect [15, 16]; C- and CP-odd (chromo-electromagnetic) backgrounds supply the system with a finite net chirality and an electric current is then induced along B. The Chiral Magnetic Effect is an interdisciplinary subject ranging over nuclear physics, astrophysics, and especially condensed matter physics in which Dirac/Weyl semimetals and graphene could provide us with clean environments under better experimental control (also applicable for the Schwinger Mechanism) [17]. So far, most of theoretical works on the Chiral Magnetic Effect are limited to homogeneous and constant E and B (see Ref. [18] for an exception), though the nucleus-nucleus collision generates electromagnetic fields with large spatial modulations [19].

So far, we have focused on the particle production in real time, but our finding of the spatially assisting mechanism due to an effective mass shift implies that the true vacuum should be modified in equilibrium. It is widely known that homogeneous and constant  $\boldsymbol{B}$  leads to the Magnetic Catalysis, i.e. enhancement of dynamical symmetry breaking or catalyzing the fermion condensate [20]. Because the mass shift shows completely the same pattern as the Chiral Gap Effect in curved space [21], we can draw the same conclusion from our calculation; spatially modulated  $\boldsymbol{B}$  increases the dynamical mass by the reorganization of the vacuum structure. To the best of our

knowledge, the present work is the very first demonstration that spatially modulated  $\boldsymbol{B}$  should assist the Magnetic Catalysis as well as the Schwinger Mechanism.

For actual calculations we employ the worldline pathintegral formalism [22], which is suited to handle pair particle production with general background fields. In this work we will not take account of back-reaction, that is, effects of additional electromagnetic fields sourced by produced charged particles, since we are interested in the production rate only for a given configuration and not the whole temporal evolutions.

Worldline Formalism: Our starting point is the (4+1)-dimensional Euclidean worldline effective action  $\Gamma_{\rm E}$  for a fermion with mass m under a given gauge configuration  $A_{\mu}(x)$ , which is generally expressed as [22]

$$\Gamma_{\rm E}[A] = \int_0^\infty \frac{dT}{T} e^{-m^2 T} \oint \mathcal{D}x$$

$$\times \exp\left\{-\int_0^T d\tau \left[\frac{1}{4} \left(\frac{dx}{d\tau}\right)^2 + ieA \cdot \frac{dx}{d\tau}\right]\right\} \Phi[A] , \quad (1)$$

$$\Phi[A] = -\frac{1}{2} \operatorname{tr} \mathcal{P} \exp\left(\frac{ie}{2} \int_0^T d\tau \, \sigma_{\mu\nu} F_{\mu\nu}\right) , \quad (2)$$

where  $\Phi[A]$  represents the spin factor with  $\sigma_{\mu\nu} \equiv \frac{1}{2} [\gamma_{\mu}, \gamma_{\nu}]$ . The Euclidean field strength tensor components are  $F_{ij} = \epsilon_{ijk} B_k$  and  $F_{4i} = -i E_i$  in terms of the physical (Minkowskian) electromagnetic fields. In the worldline formalism the auxiliary coordinate variables should satisfy the periodic boundary condition;  $x_{\mu}(0) = x_{\mu}(T)$ . It is important to note that the m-dependence appears only through  $e^{-m^2T}$  which makes the T-integration converge as long as  $m^2$  is positive.

In the present study we specifically consider a situation with the  $x_4$ -dependent E and the  $x_{1,2}$ -dependent B fields parallel to each other along the  $x_3$ -axis; i.e.  $E = E(A_4(x_{3,4}), A_3(x_{3,4}))e_3$  and  $B = B(A_1(x_{1,2}), A_2(x_{1,2}))e_3$ . In this special but topologically non-trivial situation with  $E \cdot B \neq 0$ , the electric and the magnetic parts are separable (but coupled through the T-integration) and we can express the effective action as  $\Gamma_E = -2 \int_0^\infty \frac{dT}{T} e^{-m^2 T} \mathcal{K}_E \mathcal{K}_B$ , where

$$\mathcal{K}_{E}(T; A_{3}, A_{4}) \equiv \oint \mathcal{D}x_{3}\mathcal{D}x_{4} \cos\left[\int_{0}^{T} d\tau \, eE(x)\right] 
\times \exp\left\{-\int_{0}^{T} d\tau \left[\frac{1}{4}\left(\frac{dx_{3}}{d\tau}\right)^{2} + \frac{1}{4}\left(\frac{dx_{4}}{d\tau}\right)^{2} + ieA_{3}\frac{dx_{3}}{d\tau} + ieA_{4}\frac{dx_{4}}{d\tau}\right]\right\}. (3)$$

$$\mathcal{K}_{B}(T; A_{1}, A_{2}) \equiv \oint \mathcal{D}x_{1}\mathcal{D}x_{2} \cosh\left[\int_{0}^{T} d\tau \, eB(x)\right]$$

$$\times \exp\left\{-\int_{0}^{T} d\tau \left[\frac{1}{4}\left(\frac{dx_{1}}{d\tau}\right)^{2} + \frac{1}{4}\left(\frac{dx_{2}}{d\tau}\right)^{2} + ieA_{1}\frac{dx_{1}}{d\tau} + ieA_{2}\frac{dx_{2}}{d\tau}\right]\right\}. (4)$$

The theoretical treatment of  $\mathcal{K}_E$  has been well investigated: As long as  $\mathcal{K}_B$  does not produce any exponential factor in terms of T, we can perform the T-integration approximately with the value at the stationary point  $T^*(x_{3,4})$ . Then, we can evaluate the  $x_{3,4}$ -integration with the worldline instantons  $x_{3,4}^{\text{cl}}(\tau)$  as solutions of the equations of motion [23] including Gaussian fluctuations around them to reproduce the prefactor. Finally we can just replace the magnetic part with  $\mathcal{K}_B(T^*(x_{3,4}^{\text{cl}}); A_1, A_2)$ . In this way, for constant  $E \parallel B$ , pretty straightforward calculations yield the correct answer;  $\Gamma_E = -[e^2EB/2(2\pi)^2] \coth(\pi B/E) \exp(-\pi m^2/eE)$  by picking up the n=1 instanton contribution. This can also be interpreted as a particle production rate in Minkowskian spacetime as

$$w = 2\operatorname{Im}\Gamma_{\mathcal{M}} = -2\operatorname{Re}\Gamma_{\mathcal{E}} = \frac{e^2 E B}{(2\pi)^2} \coth\left(\frac{\pi B}{E}\right) e^{-\pi m^2/eE} ,$$
(5)

which happens to coincide with the exact answer from the Euler-Heisenberg effective Lagrangian. What we will show below is that, with spatially modulated magnetic fields,  $\mathcal{K}_B$  may give rise to an exponential factor and this effectively changes  $m^2$ .

Magnetic Part with Spatial Modulation: Below we report our calculations. Let us first consider an example with the following (Sauter-type) profile of the magnetic field, the Dirac equation with which can be solved [24];

$$\mathbf{B}(x) = B \operatorname{sech}^{2}(\kappa x_{1}) \mathbf{e}_{3}.$$
 (6)

It would be more convenient to translate the functional integral into the canonical quantized representation with the corresponding Hamiltonian. Then, we can re-express  $\mathcal{K}_B$  into the following form as

$$\mathcal{K}_B = \sum_{\pm} \frac{1}{2} \operatorname{Tr} \exp(-\hat{H}_B^{\pm} T) , \qquad (7)$$

where the magnetic Hamiltonian is defined as

$$\hat{H}_B^{\pm} \equiv -\partial_1^2 - \left[\partial_2 + \frac{ieB}{\kappa} \tanh(\kappa x_1)\right]^2 \pm eB \operatorname{sech}^2(\kappa x_1) .$$
(8)

In the same way as in Ref. [24] we can find the wavefunctions to diagonalize the above Hamiltonian, and from them we can construct the eigenvalue spectrum explicitly. Specifically, the kernel takes a form of

$$\operatorname{Tr} e^{-\hat{H}_B^{\pm}T} = -\frac{1}{2\pi i} \int \frac{dp_2}{2\pi} \int_C d\lambda \, e^{-\lambda T} g^{\pm}(\lambda) \,. \tag{9}$$

Here,  $g^{\pm}(\lambda)$  is an integrated resolvent made from the wave-functions and after some calculations we find,

$$g^{\pm}(\lambda) = \tilde{g}(p_2, eB, \kappa, \lambda) \sum_{j=\pm} \psi\left(\frac{1}{2} + j\left|\frac{1}{2} \pm \frac{eB}{\kappa^2}\right| + \epsilon_- + \epsilon_+\right),$$
(10)

where we defined;  $\tilde{g}(p_2, eB, \kappa, \lambda) \equiv \kappa^4(\epsilon_- + \epsilon_+)^3/[(p_2 eB)^2 - \kappa^6(\epsilon_- + \epsilon_+)^4]$  and the dimensionless dispersion relations are  $\epsilon_\pm(\lambda) \equiv (2\kappa)^{-1} \sqrt{(p_2 \pm eB/\kappa)^2 - \lambda}$ , and  $\psi(x)$  represents the digamma function. What is necessary for our present purpose is to locate the poles of  $g^\pm(\lambda)$  and they are identified from the properties of the j=-1 digamma function. After some procedures we have discovered the explicit form of the eigenvalue spectrum as

$$\lambda_n^{\pm} = p_2^2 \left[ 1 - \frac{(eB)^2}{(\kappa^2 \tilde{n} - |\kappa^2/2 \pm eB|)^2} \right] \mp eB$$
$$-\left( \kappa^2 \tilde{n}^2 - 2\tilde{n} \left| \frac{\kappa^2}{2} \pm eB \right| + \frac{\kappa^2}{4} \right), \quad (11)$$

where a half integer  $\tilde{n} \equiv n + 1/2$  ranges with  $n \in [0, |\frac{1}{2} \pm \frac{eB}{\kappa^2}| - \frac{1}{2} - \sqrt{\frac{p_2 eB}{\kappa^3}})$  for  $\lambda_n^{\pm}$ . We can significantly simplify the above expression for  $eB > \kappa^2/2$ , which is the case for our interested situation with small inhomogeneity. Then,

$$\lambda_n^{\pm} = \left[ 1 - \frac{p_2^2 \kappa^2}{(eB - \kappa^2 n^{\pm})^2} \right] n^{\pm} (2eB - \kappa^2 n^{\pm}) , \quad (12)$$

where  $n^+=n$  and  $n^-=n+1$ . As we described before, in the presence of the electric field, the T-integral can be approximately evaluated at the stationary point and the smallest  $\lambda_n^\pm$  would dominate. Thus, we pick up the contributions from n=0 only, namely,  $\lambda_0^+=0$ . Interestingly, the second smallest eigenvalue appears from the largest  $p_2$ , which is set by the condition,  $n\geq 0$ , leading to  $\lambda_1^+\big|_{p_2=(eB-\kappa^2)/(\kappa eB)}=\lambda_0^-\big|_{p_2=(eB-\kappa^2)/(\kappa eB)}\simeq 4\kappa^2$ . Thus, the energy gap is characterized by not eB but  $\kappa^2$ .

Instead of descreasing behavior for small  $x_1$  in the Sauter-type shape, let us consider increasing behavior. One may then expect to have a negative  $\lambda_n^{\pm} \propto -\kappa^2$ . Actually, in an inhomogeneous magnetic field setup – a magnetic flux tube with finite radius – a negative-energy eigenstate was found in Ref. [25]. In view of the effective action (1), such an exponential damping factor of  $e^{\kappa^2 T}$  should be interpreted as an effective mass shift as

$$m^2 \to \tilde{m}^2 = m^2 - \kappa^2 \ . \tag{13}$$

We note that in this work we call  $\tilde{m}$  an effective mass, while we use a similar terminology, a dynamical mass, to mean a mass determined by the effective potential. We strictly distinguish them.

Now, let us confirm the above expectation by explicit calculations. For the increasing magnetic profile, for small enough  $\kappa^2$ , we can take the magnetic field and the associated vector potential as

$$\mathbf{B}(x) = \left[ B + B \frac{\kappa^2}{2} (x_1^2 + x_2^2) \right] \mathbf{e}_3 , \qquad (14)$$

$$\mathbf{A}(x) = \frac{B}{2}(x_1\mathbf{e}_2 - x_2\mathbf{e}_1) - \frac{B\kappa^2}{6}(x_1^3\mathbf{e}_2 - x_2^3\mathbf{e}_1). \quad (15)$$

Because we are interested in the most dominant exponential factor for large T, we do not have to solve the full eigenvalue spectrum but can just compute the ground state energy or the vacuum energy. We can use the standard diagrammatic technique to obtain the vacuum energy as a power series in  $\kappa^2$  from the Lagrangian,

$$L = \frac{\left(\frac{dx_1}{d\tau}\right)^2 + \left(\frac{dx_2}{d\tau}\right)^2}{4} + \frac{ieB}{2}\left(-x_2\frac{dx_1}{d\tau} + x_1\frac{dx_2}{d\tau}\right) \pm eB$$
$$\mp \frac{eB\kappa^2}{2}(x_1^2 + x_2^2) + \frac{ieB\kappa^2}{6}\left(x_2^3\frac{dx_1}{d\tau} - x_1^3\frac{dx_2}{d\tau}\right). \tag{16}$$

To the first order in  $\kappa^2$ , the first term in the second line of Eq. (16) makes a contribution of one-loop vacuum graph, which yields  $\pm \frac{1}{2}\kappa^2$ . The second term makes a contribution of two-loop vacuum graph, which yields  $-\frac{1}{2}\kappa^2$ . The sum amounts to the smallest energy of  $-\frac{1}{2}\kappa^2 - \frac{1}{2}\kappa^2 = -\kappa^2$ , which confirms the mass shift of Eq. (13). We note that, for the Sauter-type decreasing profile, the sign of  $\kappa^2$  is opposite and then the smallest energy would be  $-\frac{1}{2}\kappa^2 + \frac{1}{2}\kappa^2 = 0$  which is consistent with  $\lambda_0^+ = 0$  in Eq. (12).

Spatially Assisted Schwinger Mechanism: The evaluation of  $\mathcal{K}_E$  is a well-known computation and we quickly look over key equations here. The vector potential is supposed to have both terms of a constant electric field and a small perturbation (with  $e\varepsilon\omega\ll eE$ ) as

$$A_3(x_4) = -iEx_4 - i\varepsilon \tan(\omega x_4) . \tag{17}$$

Hereafter we use a rescaled proper time;  $\tau = Tu$ . After this rescaling, the T-dependence in  $\mathcal{K}_E$  appears only in the coefficient of  $\dot{x}_3^2 + \dot{x}_4^2$ , where  $\dot{x}_{3,4} \equiv dx_{3,4}/du$ . Because of the mass shift, the stationary point [23] is modified as  $T^* = \sqrt{\int_0^1 du \, (\dot{x}_3^2 + \dot{x}_4^2)/(2\tilde{m})}$ . Then, regardless of the concrete choice of the gauge potential, we can understand that  $\dot{x}_3^2 + \dot{x}_4^2$  is independent of u (or  $\tau$ ) from the equations of motion, namely,  $\dot{x}_3^2 + \dot{x}_4^2 = C_n^2$  and  $C_n = 2n\pi m/(eE)$  is found where n refers to the instanton number. By taking the n=1 contribution we can get  $\mathcal{K}_E$  from the corresponding instanton action, and we can eventually get the particle production rate with the dynamically assisting E and the spatially assisting E

$$w(\omega, \kappa) = \frac{e^2 E B}{(2\pi)^2} \coth\left(\frac{\pi B}{E}\right) e^{-S_{\text{inst}}(\omega, \kappa)} , \qquad (18)$$

where, for the modified Keldysh parameter  $\tilde{\gamma} \equiv \tilde{m}\omega/(eE) \geq \pi/2$ , the instanton action reads,

$$S_{\text{inst}}(\omega, \kappa) = \frac{2\tilde{m}^2}{eE} \left[ \arcsin\left(\frac{\pi}{2\tilde{\gamma}}\right) + \left(\frac{\pi}{2\tilde{\gamma}}\right) \sqrt{1 - \left(\frac{\pi}{2\tilde{\gamma}}\right)} \right]. \tag{19}$$

To have more insight, we make plots in Figs. 1 and 2 to show  $w(\omega, \kappa)$  in Eq. (18) as a function of  $\omega$  and  $\kappa$  for different E and B. It should be noted that in

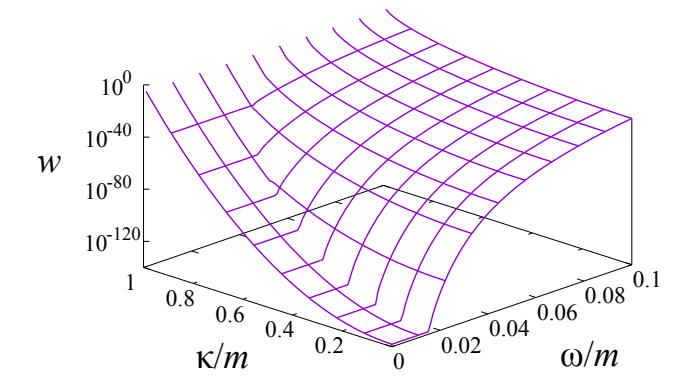


FIG. 1. Pair production rate with the dynamically assisting E with frequency  $\omega$  and the spatially assisting B with wavenumber  $\kappa$  in unit of the particle mass m, where we chose  $eE = eB = 10^{-2}m^2$ .

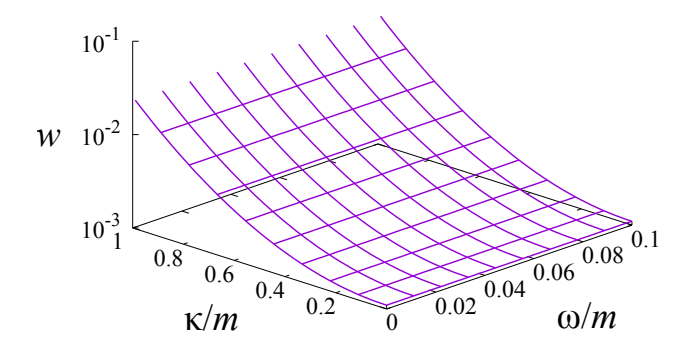


FIG. 2. The same as Fig. 1, where we chose  $eE = eB = m^2$ .

the absence of any electric field we cannot see pair production coming solely from the spatially inhomogeneous magnetic field. Strictly speaking, our expanded result makes sense under the condition,  $\kappa^2 \ll eB$ , and if  $\kappa \sim m$ and  $eE \ll m^2$  as is the case in the laser experiment, we require  $eB \gg eE$ . However, we should be aware that we can have an unexpanded result for the Sauter-type potential (6) (which will be reported in more details in a follow-up) and  $\kappa^2 \ll eB$  is not mandatory for the Spatially Assisted Schwinger Mechanism. Here, to discuss qualitative characters, we adopt eE = eB for Figs. 1 and 2. From Fig. 1 with  $eE = eB < m^2$  (which would be more relevant to the laser experiment) we see that the dynamically assisting effect has a larger slope at small  $\omega$  but gets saturated soon with increasing  $\omega$ , while the spatially assisting effect has rather opposite behavior. In contrast to this, as seen in Fig. 2 with  $eE = eB \gtrsim m^2$ (which would be more relevant to the nucleus collision experiment),  $\tilde{\gamma}$  is smaller, and the dynamically assisting effect becomes minor, but the spatially assisting effect remains prominent.

We note that standing-waves of hard X-rays could in principle realize  $\kappa \sim m_e = 511$  keV, and furthermore, in nucleus collision experiment  $\kappa$  originates from the chromo-magnetic fields whose typical scale is given by

the saturation scale  $Q_s \sim 2$  GeV (see Ref. [26] for recent reviews) that is thousands times greater than masses of quarks and gluons.

Spatially Assisted Magnetic Catalysis: An interesting question is; what happens if  $\kappa^2 > m^2$  or  $\tilde{m}^2 < 0$ ? Actually, as mentioned above, this is the case in the nucleus collision. Also in the laser experiment, such a situation could be realized by means of the Weyl/Dirac semimetals in which fermions are nearly gapless and  $\kappa^2 > m^2$  is easily achieved. It would be important to note that  $\tilde{m}^2 < 0$  is not an artifact of our approximation; in principle we could think of a massless theory for which an infinitesimal  $\kappa$  would realize  $\tilde{m}^2 < 0$ . Then, we immediately notice that the T-integration no longer converges. What is the remedy for this apparent breakdown?

We shall point out that the naive calculation of w with a fixed m should hold only transiently once we take account of interaction effects, because we then consider the particle production problem on a wrong vacuum. To illustrate this, we could have utilized an interacting fermionic model such as the Nambu–Jona-Lasinio model, but here let us give a general and thus robust argument with the Ginzburg-Landau type effective potential. For interacting fermions m should be promoted to be an inmedium mass or dynamical mass M, so that M should be self-consistently determined by the gap equation. Let us suppose that the gap equation follows from the minimum of an effective potential whose Ginzburg-Landau expansion is  $V(M^2) = a(M^2 - m_0^2)^2$  with a > 0 and  $m_0 > m$ . Then, naturally, the vacuum (ground state) should favor  $M^2 = m_0^2$  to minimize the system energy. From this point of view, a shift in Eq. (13) implies that the vacuum should be reorganized to result in an additional mass;  $M^2 = m_0^2 + \kappa^2 > m_0^2$ . Because the dynamical mass originates from a condensate of fermion and antifermion (i.e.  $\sim \langle \bar{\psi}\psi \rangle$ ), we can rephrase our finding as an enhanced condensate by finite  $\kappa$ , and this can be physically interpreted as a novel realization of the Magnetic Catalysis assisted by spatial modulation. See Ref. [21] for analogous discussions.

Spatially Assisted Chiral Magnetic Effect: A clean experimental environment for the detection of the chiral magnetic effect is a Dirac semimetal in a parallel  ${\pmb E}$  and  ${\pmb B}$  [27]. Non-zero chirality is generated by  ${\pmb E}\cdot{\pmb B}\neq 0$  according to w in Eq. (5), which together with  ${\pmb B}$  produces a topological current  $\propto wB \sim EB^2$  with an exponential suppression factor; see Ref. [10] for an explicit form. The induced current is balanced between the production rate w and the relaxation time  $\tau$ , and thus a dynamically and spatially assisted w would increase the balanced value of the topological current by an exponential factor with the residual Dirac mass replaced with the shifted one according to Eq. (13), which should be advantageous for more precise measurements of the electric conductivity.

Conclusions: The Schwinger Mechanism and the Magnetic Catalysis were explored in parallel electromagnetic fields with dynamically modulated electric and spatially modulated magnetic perturbations. We found that not only was the pair production rate enhanced with the dynamically assisting electric field but also with the spatially assisting magnetic field. The former effectively reduces the particle mass m multiplicatively, while we found that the latter reduces m subtractively. For electromagnetic fields smaller than  $m^2$ , the dynamically assisting effect is significant, whereas for electromagnetic fields comparable or larger than  $m^2$  as could be manifested in the high-energy nuclear experiment and/or in the table-top experiment with massless Dirac dispersions, the spatially assisting effect that we discovered is dominating. Our finding of the effective mass shift due to positive curvature magnetic fields is robust regardless of physical processes, so that we can apply it to a static property of the vacuum. That is, the dynamical mass for interacting fermions should be also shifted accordingly, and we discussed that spatially increasing magnetic fields should increase the dynamical mass or the condensate.

We can anticipate an intriguing application of the Spatially Assisted Schwinger Mechanism to lower the critical field strength in high-power laser facilities (in the hard X-ray region) as well as ion-laser collisions [28]. More so, it would be of paramount interest to see whether a field configuration which permits  $\kappa^2 > m^2$  is easily realized for Dirac/Weyl semimetals in appropriate optical environments. Before the vacuum reorganization is complete which takes a finite time, our results suggest that the particle production on a wrong vacuum with  $\kappa^2 > m^2$  explodes transiently, and such a transitional behavior might be related to some magnetically driven instabilities such as the Weibel and the chiral plasma instability [29].

It is of further interest to study what effects a perpendicular spatial inhomogeneity and/or a temporal modulation in the magnetic field may have. It is known that a spatially modulated electric field inhibits the pair production [6]. Also, for constant magnetic fields perpendicular to the electric field, it was found the pair production decreases [30]. These questions deserve further investigations in the future.

We are grateful to Sanjin Benić, Francois Gelis, Pablo Morales, and Igor Shovkovy for useful discussions. K. F. was partially supported by JSPS KAKENHI Grant No. 15H03652 and 15K13479.

- [4] G. V. Dunne, ELI Workshop and School on Fundamental Physics with Ultra-high Fields Monastery Frauenworth, Germany, September 29-October 2, 2008, Eur. Phys. J. D55, 327 (2009); H. Gies, Eur. Phys. J. D55, 311 (2009).
- [5] L. Keldysh, Sov. Phys. JETP **20**, 1307 (1965).
- [6] A. Nikishov, Nucl. Phys. B **21**, 346 (1970).
- [7] R. Schützhold, H. Gies, and G. Dunne, Phys. Rev. Lett. 101, 130404 (2008).
- [8] F. Hebenstreit, R. Alkofer, and H. Gies, Phys. Rev. Lett. 107, 180403 (2011), arXiv:1106.6175 [hep-ph].
- [9] A. Iwazaki, Phys. Rev. C80, 052202 (2009) arXiv:0908.4466 [hep-ph].
- [10] K. Fukushima, D. E. Kharzeev, and H. J. Warringa, Phys. Rev. Lett. 104, 212001 (2010); K. Fukushima, Phys. Rev. D92, 054009 (2015).
- [11] A. Yildiz and P. H. Cox, Phys. Rev. D 21, 1095 (1980);
  J. Ambjørn and R. J. Hughes, Annals Phys. 145, 340 (1983);
  M. Gyulassy and A. Iwazaki, Phys. Lett. B 165, 157 (1985).
- [12] D. Kharzeev, E. Levin, and K. Tuchin, Phys. Rev. C 75, 044903 (2007); N. Tanji, Annals Phys. 325, 2018 (2010).
- [13] G. S. Bali, F. Bruckmann, G. Endrdi, S. D. Katz, and A. Schäfer, JHEP 08, 177 (2014).
- [14] R. Gatto and M. Ruggieri, Lect. Notes Phys. 871, 87 (2013).
- [15] K. Fukushima, D. E. Kharzeev, and H. J. Warringa, Phys. Rev. D 78, 074033 (2008).
- [16] D. E. Kharzeev, Annals Phys. **325**, 205 (2010).
- [17] S. Vajna, B. Dóra, and R. Moessner, Phys. Rev. B 92, 085122 (2015); D. Allor, T. D. Cohen, and D. A. Mc-Gady, Phys. Rev. D 78, 096009 (2008).
- [18] H. J. Warringa, Phys. Rev. D 86, 085029 (2012).
- [19] Z. Yang, Y. Chun-Bin, C. Xu, and F. Sheng-Qin, Chin. Phys. C 39, 104105 (2015).
- [20] K. G. Klimenko, Theor. Math. Phys. 89, 1161 (1992);
  Theor. Math. Phys. 90, 1 (1992);
  V. P. Gusynin, V. A. Miransky, and I. A. Shovkovy, Phys. Rev. Lett. 73, 3499 (1994);
  I. A. Shovkovy, Lect. Notes Phys. 871, 13 (2013).
- [21] A. Flachi and K. Fukushima, Phys. Rev. Lett. 113, 091102 (2014); A. Flachi, K. Fukushima, and V. Vitagliano, Phys. Rev. Lett. 114, 181601 (2015).
- [22] C. Schubert, Phys. Rept. **355**, 73 (2001).
- [23] I. K. Affleck, O. Alvarez, and N. S. Manton, Nucl. Phys. B 197, 509 (1982); G. V. Dunne and C. Schubert, Phys. Rev. D 72, 105004 (2005).
- [24] D. Cangemi, E. D'Hoker, and G. Dunne, Phys. Rev. D 52, R3163 (1995); G. Dunne and T. Hall, Phys. Lett. B 419, 322 (1998).
- [25] M. Bordag and K. Kirsten, Phys. Rev. D 60, 105019 (1999).
- [26] F. Gelis, Int. J. Mod. Phys. E24, 1530008 (2015);
   K. Fukushima, (2016), arXiv:1603.02340 [nucl-th].
- [27] S. Borisenko, Q. Gibson, D. Evtushinsky, V. Zabolotnyy, B. Büchner, and R. J. Cava, Phys. Rev. Lett. 113, 027603 (2014); Q. Li, D. E. Kharzeev, C. Zhang, Y. Huang, I. Pletikosic, A. V. Fedorov, R. D. Zhong, J. A. Schneeloch, G. D. Gu, and T. Valla, Nat. Phys. advance online publication, (2016).
- [28] A. Di Piazza, E. Lötstedt, A. I. Milstein, and C. H. Keitel, Phys. Rev. Lett. 103, 170403 (2009).
- [29] Y. Akamatsu and N. Yamamoto, Phys. Rev. Lett. 111, 052002 (2013), arXiv:1302.2125 [nucl-th].
- [30] W. Su, M. Jiang, Z. Q. Lv, Y. J. Li, Z. M. Sheng, R. Grobe, and Q. Su, Phys. Rev. A 86, 013422 (2012).

<sup>[1]</sup> S. K. Lamoreaux, Rept. Prog. Phys. 68, 201 (2005).

J. Schwinger, Phys. Rev. 82, 664 (1951); F. Sauter, Z. Phys. 69, 742 (1931); W. Heisenberg and H. Euler, Z. Phys. 98, 714 (1936).

<sup>[3]</sup> G. V. Dunne, Heisenberg-Euler effective Lagrangians: Basics and extensions (2004) hep-th/0406216.